

**$^{57}\text{Fe}$  Mössbauer spectroscopy studies of  $\text{CaFe}_4\text{As}_3$** 

I. Nowik and I. Felner

*Racah Institute of Physics, Hebrew University, Jerusalem, 91904, Israel*

A. B. Karki and R. Jin\*

*Department of Physics and Astronomy, Louisiana State University, Baton Rouge, Louisiana 70803, USA*

(Received 29 July 2011; revised manuscript received 5 September 2011; published 7 December 2011)

We report on the  $^{57}\text{Fe}$  Mössbauer spectroscopy and direct-current magnetization studies of orthorhombic  $\text{CaFe}_4\text{As}_3$ , which undergoes two magnetic transitions with the formation of spin density wave at  $T_{N1} = 88$  K (incommensurate) and  $T_{N2} = 26$  K (commensurate). The magnetic Mössbauer spectroscopy spectra below  $T_{N1}$  are composed of four subspectra attributed to the four in-equivalent Fe crystallographic sites: three Fe ions in the divalent state ( $\text{Fe}^{2+}$ ) and one as  $\text{Fe}^{1+}$ . However, the magnetic lines are much broader than that below  $T_{N2}$ , indicating an incommensurate magnetic state. In the paramagnetic state, the Mössbauer spectroscopy spectra are composed of three doublets; one of them is related to  $\text{Fe}^{1+}$ . Evidence for spin fluctuations above  $T_{N1}$  is observed.

DOI: [10.1103/PhysRevB.84.212402](https://doi.org/10.1103/PhysRevB.84.212402)

PACS number(s): 76.80.+y, 74.70.Xa, 75.50.Ee, 75.30.Fv

**I. INTRODUCTION**

Recently, attention has been focused on the research of Fe-based materials, because they reveal superconductivity with transition temperature comparable to cuprates. The building block of these materials is either a Fe-As or a Fe-Se layer formed by edge-shared  $\text{FeAs}_4$  or  $\text{FeSe}_4$  tetrahedra. Before chemical doping or application of pressure in so-called parent compounds, these Fe-As or Fe-Se layers exhibit long-range three-dimensional antiferromagnetic (AFM) spin density wave (SDW) order at  $T_N \approx 140 - 150$  or  $520 - 550$  K with a  $\text{Fe}^{2+}$  moment of  $0.87(3)$  or  $3.31 \mu_B/\text{Fe}$ , respectively.<sup>1,2</sup> In  $\text{BaFe}_2\text{As}_2$ , the Fe moments are aligned within the  $ab$  plane,<sup>1</sup> whereas neutron powder diffraction (NPD) shows that they are along the  $c$  axis in  $\text{KFe}_2\text{Se}_2$ .<sup>2</sup> The major difference between the two systems, noticeable from several types of measurements, is that the temperature–composition phase diagrams show generic behavior as a function of the substituent concentration  $x$  in the Fe-As-based materials. This implies a systematic *suppression* of the magnetic transition by increasing  $x$  or pressure. Then, above a critical concentration (which depends on the substituent), superconductivity is observed.<sup>3,4</sup> On the other hand, the nonstoichiometric  $\text{A}_z\text{Fe}_{2-y}\text{Se}_2$  also becomes superconducting  $\sim 30 - 33$  K, but the AFM state persists even at low temperatures.<sup>5,6</sup> This means that in  $\text{A}_z\text{Fe}_{2-y}\text{Se}_2$ , there is a *coexistence* of magnetism and superconductivity, since both states are confined to the same Fe-Se crystallographic layer.<sup>5</sup> This makes the extensive search for new Fe-As-based compounds inseparable from the search of new high- $T_c$  superconducting materials.

The new compound  $\text{CaFe}_4\text{As}_3$  is a good reference, as it has the same building block as Fe-As-based superconducting compounds, i.e., edge-shared  $\text{FeAs}_4$  tetrahedron.  $\text{CaFe}_4\text{As}_3$  crystallizes in the orthorhombic structure (space group  $Pnma$ ) with  $a = 11.873 \text{ \AA}$ ,  $b = 3.740 \text{ \AA}$ , and  $c = 1.574 \text{ \AA}$ ,<sup>7</sup> as reported in Ref. 8 and illustrated in Fig. 1. NPD studies show four independent Fe sites in the crystallographic unit cell, all of the multiplicity 4 and in the  $(x, 1/4, z)$  positions, as reported in Ref. 8. Electric resistivity, magnetic susceptibility, and specific heat studies reveal the existence of two transitions.<sup>9–11</sup> One is the formation of an incommensurate SDW along the  $b$

axis below  $T_{N1} \approx 88$  K, and the other is the change to a commensurate SDW in the  $ac$  plane below  $T_{N2} \approx 26$  K.<sup>8</sup>

Mössbauer spectroscopy (MS) of  $^{57}\text{Fe}$  isotope seems particularly useful for studying  $\text{CaFe}_4\text{As}_3$  system, because Fe makes the basic constituent of this compound. Formal charges of the various Fe ions can be assigned by assuming a complete electron transfer from the Ca and Fe cations to the As anions. To naturalize the unit cell charge, the formal Fe valences are three  $\text{Fe}^{2+}$  and one  $\text{Fe}^{1+}$  for  $\text{Ca}^{2+}$  and  $\text{As}^{3-}$ . Indeed, the room temperature MS study exhibits approximately two paramagnetic quadrupole subspectra with isomer shifts (ISs) of  $0.32(1)$  and  $0.54(1)$  mm/s and an intensity ratio of 3:1, thus confirming the presence of the two Fe states.<sup>6</sup> Moreover, the substitution of Cr for Fe measured by NPD and MS show, selectively, Cr occupation in the  $\text{Fe}_4$  site, which is attributed to the  $\text{Fe}^{1+}$  site.<sup>12</sup>

Our focus in this Brief Report is the comprehensive  $^{57}\text{Fe}$  MS studies of  $\text{CaFe}_4\text{As}_3$  in both commensurate and incommensurate magnetic states, as well as in the paramagnetic region. In the paramagnetic region, the MS spectra are actually composed of three subspectra (intensities 2:1:1) and attributed to three  $\text{Fe}^{2+}$  and one  $\text{Fe}^{1+}$ , as identified by their ISs. Below  $T_{N1}$ , the MS are composed of four subspectra associated with the four in-equivalent Fe sites. In the commensurate region, the lines of all subspectra are much sharper than that in the incommensurate region.

**II. EXPERIMENTAL DETAILS**

Single crystals of  $\text{CaFe}_4\text{As}_3$  were grown out of Sn flux. The detailed procedure is described in Ref. 9. These crystals were ground into powder for measurements reported here. Zero-field-cooled (ZFC) temperature dependence of the magnetization measured under various applied fields was performed in a commercial MPMS5 Quantum Design superconducting quantum interference device (SQUID) magnetometer. Before recording the ZFC curve, the SQUID magnetometer was adjusted to be in “real”  $H = 0$  state. The  $^{57}\text{Fe}$  Mössbauer studies of powder  $\text{CaFe}_4\text{As}_3$  at temperatures of 5–297 K were performed using a conventional constant acceleration drive

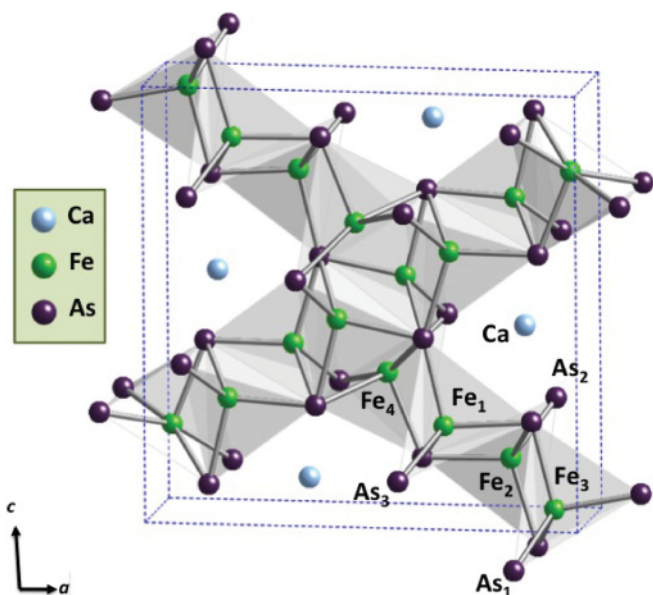


FIG. 1. (Color online) Crystallographic structure of  $\text{CaFe}_4\text{As}_3$  with indication of four Fe sites.

in transmission mode, in conjunction with a 50-mCi  $^{57}\text{Co}:\text{Rh}$  source. The absorber was cooled to low temperatures in a Janis model SHI-850-5 closed cycle refrigerator. The spectra were analyzed in terms of least square fit procedures to theoretical expected spectra. The velocity calibration was done by the spectrum of an  $\alpha$ -iron foil. The reported ISs are relative to this foil.

### III. EXPERIMENTAL RESULTS

Figure 2 shows the temperature dependence of magnetization ( $M$ ) measured in the ZFC mode at 15 Oe for  $\text{CaFe}_4\text{As}_3$  powder. The complicated temperature dependence of  $M$  is similar to that reported in Ref. 7. The pronounced peak at  $T_{N2} = 26$  K, the bent at  $T_{N1} = 88$  K, and a broad plateau at 88–112 K are readily observed. The isothermal field dependence of the magnetizations  $M(H)$  measured at 5 and 140 K are

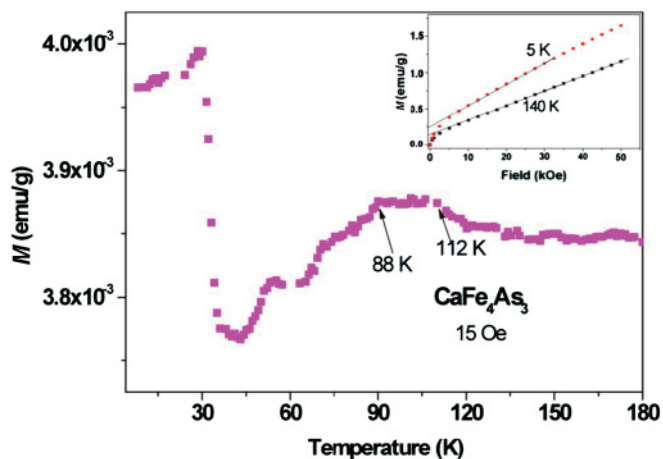


FIG. 2. (Color online) Temperature dependence of magnetization of  $\text{CaFe}_4\text{As}_3$  powder measured at 15 Oe in ZFC mode. The isothermal magnetizations at 5 and 140 K are shown in the inset.

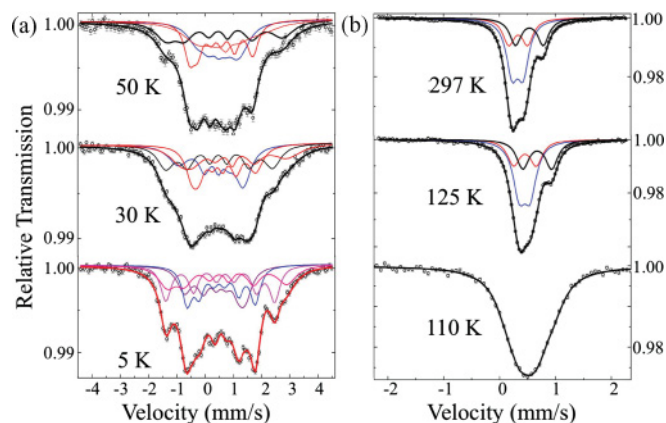


FIG. 3. (Color online) Mössbauer spectra of  $\text{CaFe}_4\text{As}_3$  (a) below and (b) above  $T_{N1} = 88$  K. Notice the different scales.

presented in the inset. Both  $M(H)$  curves are not linear at low  $H$ . The linear part at 5 K reflects the AFM nature of the sample, and the slope obtained is  $\sim 0.0135$  emu/mole Oe. In the paramagnetic range, the slope is  $\sim 0.0101$  emu/mole Oe. The extrapolated values to  $H = 0$  are 0.23 and 0.13 emu/g for  $T = 5$  and 140 K, respectively. This means that a small fraction of a ferromagnetic extra phase is present, probably 0.06% – 0.1% of Fe, not detectable by x-ray diffraction and/or by MS. Above  $\sim 350$  K, the compound follows the Curie-Weiss law.<sup>9</sup>

$^{57}\text{Fe}$  MS studies of  $\text{CaFe}_4\text{As}_3$  at a range of temperatures have been performed. Figure 3 shows the MS of  $\text{CaFe}_4\text{As}_3$  below [Fig. 3(a)] and above [Fig. 3(b)]  $T_{N1}$ . The hyperfine parameters deduced are summarized in Tables I and II. Because of the higher resolution in our spectra in comparison to those reported in Refs. 7 and 12, we are confident that in the paramagnetic range (at 125 K and at room temperature), the spectra display *three* pure quadrupole spectra with a common line width of 0.263 mm/s and intensity ratio 2:1:1 (Fig. 3). It seems that two of the  $\text{Fe}^{2+}$  sites are indistinguishable and have almost the same hyperfine parameters. The first two subspectra have similar IS (0.32 and 0.33 mm/s at 297 K) corresponding to  $\text{Fe}^{2+}$  but possess different quadrupole interactions  $EQ (= \frac{1}{4}e^2qQ)$  (Table I). The hyperfine parameters of the third subspectrum are much larger: IS = 0.535 mm/s, and  $EQ = 0.248$  mm/s, which may correspond to  $\text{Fe}^{1+}$ .<sup>6</sup> The larger IS values at 125 K, relative to that obtained at 297 K, are due to the thermal shift as expected.

As can be seen in Fig. 3, the spectra display four equally intense subspectra (fixed intensity ratios) below  $T_{N1}$ , revealing additional magnetic splitting with distributions in hyperfine fields ( $H_{\text{eff}}$ ), which is typical to SDW Mössbauer spectra.

TABLE I. Isomer Shift (IS) and quadrupole splitting (EQ) of  $\text{CaFe}_4\text{As}_3$  in the paramagnetic state.

$T$ (K)		$2\text{Fe}^{2+}$	$\text{Fe}^{2+}$	$\text{Fe}^{1+}$
125	IS (mm/s)	0.45(1)	0.45(1)	0.67(1)
	EQ (mm/s)	0.10(1)	0.20(1)	0.26(1)
297	IS (mm/s)	0.32(1)	0.33(1)	0.53(1)
	EQ (mm/s)	0.10(1)	0.17(1)	0.25(1)

TABLE II. IS, effective quadrupole interactions ( $EQ_{\text{eff}} = EQ \times \frac{1}{2}(3 \cos^2(\Theta) - 1)$  (where  $\Theta$  is the angle between the hyperfine field and the axis of the local electric field gradient responsible for the quadrupole interaction), the magnetic hyperfine field ( $H_{\text{eff}}$ ) of  $\text{CaFe}_4\text{As}_3$  in the magnetic states, and the magnetic moment amplitudes  $M_s$  obtained from NPD studies (Ref. 8).

$T$ (K)		$\text{Fe}_1$	$\text{Fe}_2$	$\text{Fe}_3$	$\text{Fe}_4$ ( $\text{Fe}^{1+}$ )
5	IS (mm/s) $\pm$ 0.01	0.50	0.55	0.37	0.81
	$EQ_{\text{eff}}$ (mm/s) $\pm$ 0.01	0.03	0.08	-0.24	0.13
	$H_{\text{eff}}$ (T) $\pm$ 0.2	11.6	7.2	7.5	11.5
	$M_s$ ( $\mu_B$ ) at 1.5 K	2.14	1.55	1.83	1.94
30	IS (mm/s) $\pm$ 0.01	0.48	0.55	0.43	0.84
	$EQ_{\text{eff}}$ (mm/s) $\pm$ 0.01	0.01	0.11	-0.20	0.18
	$H_{\text{eff}}$ (T) $\pm$ 0.2	11.7	7.0	7.2	11.6
	$M_s$ ( $\mu_B$ ) at 30 K	1.40	1.61	1.67	1.84

All subspectra were fitted with a fixed common line width of 0.284 mm/s. While the resolution of the separate absorption lines is reasonable at 5 K (below  $T_{N2}$ , the commensurate SDW region), the spectra become much worse at  $T_{N2} < T < T_{N1}$  (the incommensurate SDW region), even though they display little change in total width. The observed four  $H_{\text{eff}}$  values in Table II are caused by four in-equivalent Fe sites. At 5 K, the largest IS = 0.805 mm/s (in comparison with the others with ISs of less than 0.547 mm/s) is attributed to  $\text{Fe}_4$  ( $\text{Fe}^{1+}$ ), following the assignment done in Refs. 8 and 12. The higher IS value at 5 K relative to that obtained at room temperature results from (as expected) the second-order Doppler effect. From the  $H_{\text{eff}}$  values obtained at 5 K, we deduce the saturated magnetic moment ( $M_s$ ) acting on the Fe ions at low temperatures. In general,  $H_{\text{eff}}$  is proportional to the magnetic moment  $M_s$ . Therefore, the  $H_{\text{eff}}$  values obtained are attributed to the  $M_s$  of the four sites deduced from NPD.<sup>8</sup> The constant of proportionality,  $\beta = H_{\text{eff}}/M_s$ , is  $\sim 6T/\mu_B$  in the present case. This value is much smaller than that obtained for Fe or  $\text{Fe}_2\text{O}_3$  ( $\sim 11 - 15T/\mu_B$ ) and is consistent with the conclusion made in Ref. 13. According to Ref. 13,  $\beta$  depends on various parameters; thus, the scaling of  $H_{\text{eff}}$  and  $M_s$  is not unique. The spectrum obtained at 50 K is quite similar to that of 30 K (Fig. 3). As it is in the incommensurate SDW state, the hyperfine values deduced at 50 K are not conclusive and therefore are not included in Table II. On the other hand, magnetic spin fluctuations exist above  $T_{N1} = 88$  K. Figure 3 shows a broader spectrum at 110 K, compared to the spectra at 125 K and room temperature. This is consistent with the broad maximum observed in magnetization (Fig. 2).

As far as the MS studies are concerned, we compare the magnetic properties of  $\text{CaFe}_4\text{As}_3$  to the two related SDW

$\text{BaFe}_2\text{As}_2$  and  $\text{KFe}_2\text{Se}_2$  compounds, in which the Fe ions reside in one crystallographic site only. The various shapes of the SDW state for the  $\text{BaFe}_2\text{As}_2$  system are discussed in detail in Ref. 14.  $\text{BaFe}_2\text{As}_2$  is magnetically ordered at  $T_N = 136(1)$  K, with  $\text{Fe}^{2+}$  moments of  $0.87(3) \mu_B/\text{Fe}$  aligned within the basal plane.<sup>1</sup> Below  $T_N$ , all our MS spectra of  $\text{BaFe}_2\text{As}_2$  were analyzed in terms of a superposition of commensurate and incommensurate SDW subspectra with an average  $H_{\text{eff}}$  ( $5.53 \pm 0.6$  T at 5 K).<sup>15</sup> Thus,  $\beta = 6.3$  T/ $\mu_B$  was obtained and is similar to that of  $\text{CaFe}_4\text{As}_3$ . However,  $\text{KFe}_2\text{Se}_2$  is AFM ordered up to  $\sim 520$  K, with  $\text{Fe}^{2+}$  moments of  $3.31 \mu_B/\text{Fe}$ , which forms a collinear AFM structure along the  $c$  axis.<sup>2</sup> Our MS studies show clearly that  $H_{\text{eff}} = 28.1$  T at 93 K. In contrast to Ref. 2, the best fit to the experimental data is obtained only when the Fe moments are tilted by  $\theta \approx 44^\circ$  from the  $c$  axis.<sup>16</sup> For  $\text{KFe}_2\text{Se}_2$ , the ratio  $\beta = 8.5$  T/ $\mu_B$ . Again, this proves that the scaling of  $H_{\text{eff}}$  and  $M_s$  is not unique, as proposed in Ref. 13.

Another point of interest is the high IS obtained (0.81 mm/s at 5 K) for one subspectrum of  $\text{CaFe}_4\text{As}_3$ , which is attributed to  $\text{Fe}^{1+}$  ( $\text{Fe}_4$  site). Such a state is seldom observed. As stated previously, one Fe ion must be in a lower formal valence, and the remaining three Fe ions are in the divalent state to preserve neutrality of  $\text{CaFe}_4\text{As}_3$ . High-spin  $\text{Fe}^{1+}$  is not found in stable compounds, but its existence has been shown as a substitutional impurity in good insulating ionic lattices, as transients after radioactive decay as observed for  $^{57}\text{Co}$  decay in  $\text{TiO}_2$ ,<sup>17</sup>  $\text{MgO}$ , or  $\text{CaO}$  or when  $^{57}\text{CoCl}_2$  is doped into  $\text{KCl}$ .<sup>18,19</sup> The stable  $\text{Fe}^{1+}$  state is observed in a compact *metallic* system; this is unique and deserves further study. Further experimental and theoretical work is needed to establish its entire physical and chemical properties.

#### IV. CONCLUSIONS

The four in-equivalent Fe ions in  $\text{CaFe}_4\text{As}_3$  undergo two magnetic transitions: (1) an incommensurate SDW order of the Fe ions below  $T_{N1} = 88$  K and (2) a commensurate AFM structure below  $T_{N2} \approx 26$  K. Our  $^{57}\text{Fe}$  MS indicates the relative large IS and EQ hyperfine parameters of one subspectrum in the paramagnetic range. This is attributed to the presence of a *stable*  $\text{Fe}^{1+}$ , a seldom-observed state.

#### ACKNOWLEDGMENTS

We thank G. T. McCandless for drawing the structure of  $\text{CaFe}_4\text{As}_3$  in Fig. 1. The research in Jerusalem is supported by the Israel Science Foundation (Bikura 459/09) and by the joint German-Israeli Project Cooperation (DIP). The work at Louisiana State University is supported by the US National Science Foundation under Grant No. DMR-1002622 (R.J.).

\*rjin@lsu.edu

<sup>1</sup>Q. Huang, Y. Qiu, Wei Bao, M. A. Green, J. W. Lynn, Y. C. Gasparovic, T. Wu, G. Wu, and X. H. Chen, *Phys. Rev. Lett.* **101**, 257003 (2008).

<sup>2</sup>P. Zavalij, W. Bao, X. F. Wang, J. J. Ying, X. H. Chen, D. M. Wang, J. B. He, X. Q. Wang, G. F. Chen, P.-Y. Hsieh, Q. Huang, and M. A. Green, *Phys. Rev. B* **83**, 132509 (2011).

- <sup>3</sup>N. Ni, A. Thaler, J. Q. Yan, A. Kracher, E. Colombier, S. L. Bud'ko, and P. C. Canfield, *Phys. Rev. B* **82**, 024519 (2010).
- <sup>4</sup>A. P. Dioguardi, N. Roberts-Warren, A. C. Shockley, S. L. Bud'ko, N. Ni, P. C. Canfield, and N. J. Curro, *Phys. Rev. B* **82**, 140411(R) (2010).
- <sup>5</sup>R. H. Liu, X. G. Luo, M. Zhang, A. F. Wang, J. J. Ying, X. F. Wang, Y. J. Yan, Z. J. Xiang, P. Cheng, G. J. Ye, Z. Y. Li, and X. H. Chen, *Europhys. Lett.* **94**, 27008 (2011).
- <sup>6</sup>Z. Shermadini, A. Krzton-Maziopa, M. Bendele, R. Khasanov, H. Luetkens, K. Conder, E. Pomjakushina, S. Weyeneth, V. Pomjakushin, O. Bossen, and A. Amato, *Phys. Rev. Lett.* **106**, 117602 (2011).
- <sup>7</sup>I. S. Todorov, D. Y. Chung, C. D. Malliakas, Q. Li, T. Bakas, A. Douvalis, G. Trimarchi, K. Gray, J. F. Mitchel, A. R. Freeman, and M. G. Kanatzidis, *J. Am. Chem. Soc.* **131**, 5405 (2009).
- <sup>8</sup>P. Manuel, L. C. Chapon, I. S. Todorov, D. Y. Chung, J.-P. Castellán, S. Rosenkranz, R. Osbron, P. Toledano, and M. G. Kanatzidis, *Phys. Rev. B* **81**, 184402 (2010).
- <sup>9</sup>A. B. Karki, G. T. McCandless, S. Stadler, Y. M. Xiong, J. Li, J. Y. Chan, and R. Jin, *Phys. Rev. B* **84**, 054412 (2011).
- <sup>10</sup>L. Zhao, T. Yi, J. C. Fettinger, S. M. Kauzlarich, and E. Morosan, *Phys. Rev. B* **80**, 020404 (2009).
- <sup>11</sup>M. S. Kim, Z. P. Yin, L. L. Zhao, E. Morosan, G. Kotliar, and M. C. Aronson, *Phys. Rev. B* **84**, 075112 (2011).
- <sup>12</sup>I. S. Todorov, D. Y. Chung, H. Claus, K. Gray, Q. Li, J. Schleuter, T. Bakas, A. P. Douvalis, M. Gutmann, and M. G. Kanatzidis, *Chem. Mater.* **22**, 4996 (2010).
- <sup>13</sup>S. M. Dubil, *J. Alloys Compd.* **448**, 18 (2009).
- <sup>14</sup>A. Blachowski, K. Ruebenbauer, J. Zukrowski, K. Rogacki, Z. Bukowski, and J. Karpinski, *Phys. Rev. B* **83**, 134410 (2011).
- <sup>15</sup>I. Nowik, I. Felner, N. Ni, S. L. Bud'ko, and P. C. Canfield, *J. Phys. Condens. Matter* **22**, 355701 (2010).
- <sup>16</sup>I. Nowik, I. Felner, M. Zhang, A. F. Wang, and X. H. Chen, *Supercond. Sci. Technol.* **24**, 095015 (2011).
- <sup>17</sup>K. Ruebenbauer, U. D. Wdowik, M. Kwater, and J. T. Kowalik, *Phys. Rev. B* **54**, 12880 (1996).
- <sup>18</sup>J. Chappert, R. B. Frankel, and N. A. Blum, *Phys. Lett.* **25A**, 149 (1967).
- <sup>19</sup>J. G. Mullen, *Phys. Rev.* **131**, 1415 (1963).